Wiley Online Library
Early View publication on www.wileyonlinelibrary.com
(issue and page numbers not yet assigned;
citable using Digital Object Identifier – **DOI**)

Phys. Status Solidi C, 1–4 (2016) / **DOI** 10.1002/pssc.201510166

physica status solidi c
www.pss-c.com
current topics in solid state physics

Molecular beam epitaxy of free-standing bulk wurtzite $Al_xGa_{1-x}N$ layers using a highly efficient RF plasma source

S. V. Novikov[*,1], **C. R. Staddon**[1], **S.-L. Sahonta**[2], **R. A. Oliver**[2], **C. J. Humphreys**[2], and **C. T. Foxon**[1]

[1] School of Physics and Astronomy, University of Nottingham, Nottingham NG7 2RD, UK
[2] Department of Materials Science and Metallurgy, University of Cambridge, Cambridge, CB3 0FS, UK

Received 21 September 2015, revised 4 January 2016, accepted 28 January 2016

Keywords molecular beam epitaxy, semiconducting III-V materials, nitrides, substrates

---

* Corresponding author: e-mail sergei.novikov@nottingham.ac.uk, Phone: +44 115 951 5138, Fax: +44 115 951 5180

Recent developments with group III nitrides suggest $Al_xGa_{1-x}N$ based LEDs can be new alternative commercially viable deep ultra-violet light sources. Due to a significant difference in the lattice parameters of GaN and AlN, $Al_xGa_{1-x}N$ substrates would be preferable to either GaN or AlN for ultraviolet device applications. We have studied the growth of free-standing wurtzite $Al_xGa_{1-x}N$ bulk crystals by plasma-assisted molecular beam epitaxy (PA-MBE) using a novel RF plasma source. Thick wurtzite $Al_xGa_{1-x}N$ films were grown by PA-MBE on 2-inch GaAs (111)B substrates and were removed from the GaAs substrate after growth to provide free standing $Al_xGa_{1-x}N$ samples. Growth rates of $Al_xGa_{1-x}N$ up to 3 μm/h have been demonstrated. Our novel high efficiency RF plasma source allowed us to achieve free-standing bulk $Al_xGa_{1-x}N$ layers in a single day's growth, which makes our MBE bulk growth technique commercially viable.

1 Introduction Currently there is a high level of interest in the development of ultraviolet (UV) light sources for solid-state lighting, optical sensors, surface decontamination and water purification. III-V semiconductor UV LEDs are now successfully manufactured using the $Al_xGa_{1-x}N$ material system. The majority of UV LEDs require $Al_xGa_{1-x}N$ layers with compositions in the mid-range between AlN and GaN. For example for efficient water purification such $Al_xGa_{1-x}N$ LEDs need to emit in the wavelength range 250-280 nm [1]. However, there is a significant difference in the lattice parameters of GaN and AlN [1]. Therefore $Al_xGa_{1-x}N$ substrates would be preferable to those of either GaN or AlN for many ultraviolet device applications. This has stimulated a search for methods to produce bulk $Al_xGa_{1-x}N$ crystals with variable AlN content [2, 3].

MBE is normally regarded as an epitaxial technique for the growth of very thin layers with monolayer control of their thickness. However, we have used the MBE technique for bulk crystal growth and have produced free-standing layers of zinc-blende GaN up to 100 μm in thickness [4]. We have also demonstrated the scalability of the process by growing free-standing zinc-blende GaN layers up to 3-inches in diameter. Our newly developed PA-MBE process for the growth of bulk zinc-blende GaN layers can also be used to achieve free-standing wurtzite $Al_xGa_{1-x}N$ wafers [5]. Thick wurtzite $Al_xGa_{1-x}N$ films with an AlN content, x, from 0 to 0.5 were successfully grown by PA-MBE on 2-inch GaAs (111)B substrates. However, in our previous studies the growth rate for $Al_xGa_{1-x}N$ films remained below 1 μm/h and this is too slow to make the process commercially viable. We need to increase the growth rate and decrease the growth time required to achieve free-standing bulk $Al_xGa_{1-x}N$ layers to less than 1 day.

A few years ago Riber developed a novel plasma source for the fast growth of GaN layers - RF-N 50/63. Riber have modified the construction of the source and optimised the design of pyrolytic boron nitride (PBN) crucible and PBN aperture arrangement. The conductance of the aperture plate has been increased by increasing the number of 0.3 mm diameter holes to 1200. The first tests of the novel Riber source were performed for the growth of very thin GaN layers grown for 5 min on small size wafers [6]. The authors of that work demonstrated that with this novel source it was possible to achieve GaN growth rates up to 2.65 µm/h [6]. We have successfully used similar type Riber plasma source to demonstrate growth rates of thick GaN layers up to 1.8 µm/h on 2-inch diameter GaAs (111)B and sapphire wafers [7].

Recently, Riber have modified the design of the aperture of their plasma source for even faster growth of GaN layers. The aperture conductance has been increased by increasing the number of holes, which allows a further increase in the GaN growth rate. Researchers from Santa Barbara have demonstrated that the new source with 5880 holes in the aperture plate allows them to achieve growth rates for thin GaN layers up to 7.6 µm/h with high nitrogen flow rates of about 25 sccm [8].

In this paper we will describe our recent results in the development of our PA-MBE approach for the growth of free-standing wurtzite $Al_xGa_{1-x}N$ bulk crystals using the latest model of fast-growth Riber RF plasma source with the 5880 hole aperture plate.

2 Experimental details

Wurtzite (hexagonal) GaN and $Al_xGa_{1-x}N$ layers were grown on different substrates by plasma-assisted molecular beam epitaxy (PA-MBE) in a MOD-GENII system [4, 5]. 2-inch diameter sapphire and GaAs (111)B substrates were used. The active nitrogen for the growth of the group III-nitrides was provided by RF activated plasma sources. We compared different nitrogen plasma sources for the growth of thick wurtzite GaN and $Al_xGa_{1-x}N$ films including a standard HD25 plasma source from Oxford Applied Research and a modified novel high efficiency plasma source from Riber RF-N 50/63 with the 5880 hole aperture plate.

We have used an As_2 flux of ~6 10^{-6} Torr during substrate heating and removal of oxide on GaAs (111)B substrates. The aim was to prevent any thermal degradation and roughening of the GaAs substrate surface. The arsenic flux was terminated at the start of the GaN and $Al_xGa_{1-x}N$ growth.

A thin GaN buffer was deposited before the growth of the $Al_xGa_{1-x}N$ layers of the desired composition. Bulk $Al_xGa_{1-x}N$ layers were grown under strongly group III-rich conditions in order to achieve the best structural quality layers [9]. In the current study the $Al_xGa_{1-x}N$ layers were grown at temperatures of ~700 ^{o}C. We are not able to use higher growth temperatures due to low thermal stability of the GaAs wafers in vacuum above ~700 ^{o}C.

Thick $Al_xGa_{1-x}N$ layers were grown by MBE on GaAs substrates and the GaAs was subsequently removed using a chemical etch (20 ml H_3PO_4 : 100 ml H_2O_2) in order to produce free-standing $Al_xGa_{1-x}N$ wafers. We have achieved $Al_xGa_{1-x}N$ layers with thicknesses up to 100 µm. From our previous experience with MBE growth of bulk zinc-blende and wurtzite $Al_xGa_{1-x}N$ [4, 5], such thicknesses are sufficient to obtain free-standing $Al_xGa_{1-x}N$ layers.

The structural properties of the samples were studied in-situ using reflection high-energy electron diffraction (RHEED) and after growth ex-situ measurements were performed using X-ray diffraction (XRD) and transmission electron microscopy (TEM). The Philips X'Pert MRD diffractometer was used for XRD analysis of the layers.

Advanced transmission electron microscopy (TEM) studies were performed using a JEOL 4000 EX microscope operating at 400 kV. Specimens were prepared for TEM by mechanical polishing, dimple grinding and ion milling with an argon ion acceleration voltage of 4 kV.

We have studied Al incorporation in the $Al_xGa_{1-x}N$ layers by secondary ion mass spectrometry (SIMS) using Cameca IMS-3F and IMS-4F systems and Oxford Instruments EDX system.

3 Results and discussion

At the first stage we carried out PA-MBE growth of thin (~1 µm) wurtzite $Al_xGa_{1-x}N$ layers on two-inch diameter (111)B GaAs substrates. This substrate orientation was chosen in order to initiate the growth of the hexagonal phase of material. Wurtzite GaN buffers, ~50 nm thick, were deposited before the growth of all the $Al_xGa_{1-x}N$ layers. The HD25 plasma source from Oxford Applied Research and a modified novel high efficiency plasma source from Riber were compared for the initiation of GaN on (111)B GaAs substrates. For both RF plasma sources we have observed a hexagonal GaN RHEED pattern a few minutes into the growth.

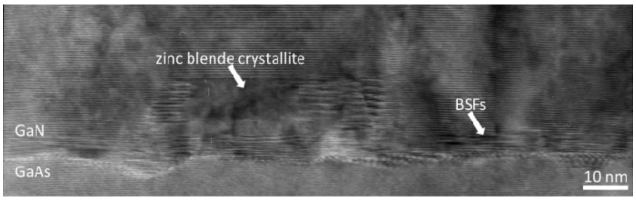

Figure 1 TEM image of a GaN layer–GaAs (111) B substrate interface.

In order to study the GaN/GaAs interface in more detail, we have performed high-resolution TEM. Zinc-blende crystallites have been observed at the GaN layer/GaAs (111)B substrate interface as shown in Fig. 1. Zinc-blende crystallites extend for the first few tens of nanometres into the GaN wurtzite film, before being terminated at (0001) basal plane stacking faults. It is well known that arsenic can be used to force the growth of metastable zinc-blende (cubic) GaN layers and we have successfully used that for the growth of our zinc-blende layers [4]. Therefore, a small fraction of zinc-blende GaN close to the interface may be explained by As contamination of the first nanometers of the GaN layer. We have also observed some erosion of the GaAs substrate surface. There may be two main reasons for the roughening of the GaAs interface – it may be a result of the initial N-plasma etching or it may be a result of Ga-melt etching due to the relatively high As solubility in Ga at MBE growth temperatures. We still have not resolved which of these mechanisms is dominant.

For thin $Al_xGa_{1-x}N$ layers grown with both RF plasma sources with increasing Al content we observed a gradual shift of the position of the $Al_xGa_{1-x}N$ XRD peak in 2θ-ω plots to higher angle. As expected both PL and CL studies confirmed an increase of the band gap of $Al_xGa_{1-x}N$ layers with increasing Al content.

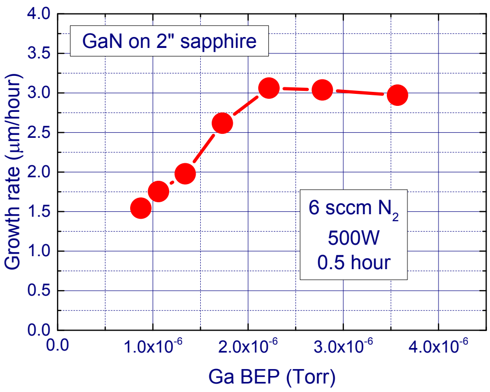

Figure 2 Growth rate dependence for GaN layers on 2-inch sapphire on the Ga flux for the Riber plasma source with 5880 holes in the aperture plate.

Based on these results we then grew thick wurtzite $Al_xGa_{1-x}N$ layers under similar growth conditions using the novel Riber source with 5880 holes in the aperture plate. Previous studies demonstrated that to achieve the highest growth rate of ~7.6 μm/h one needs to use a very high nitrogen flow of ~25 sccm [8]. In order to grow thick $Al_xGa_{1-x}N$ layers in our conventional MBE system with the standard pumping configuration we used relatively low nitrogen flow rates of ~6 sccm. That enabled us to grow thick $Al_xGa_{1-x}N$ layers with our CT-8 cryopump pumping system without frequent regeneration of the cryopump. The beam equivalent nitrogen pressure in the chamber during growth did not exceed 1×10^{-4} Torr.

Initially we have grown thick GaN layers on 2-inch sapphire (0001) wafers to establish the transition point from N-rich to Ga-rich MBE growth [9]. The GaN layers were grown for 0.5 h with a nitrogen flow of 6 sccm and with a fixed RF power of 500 W. Figure 2 shows the dependence of the growth rate for GaN layers grown with different Ga fluxes. We measured the thickness of the GaN layers after growth by an optical interference method. Under N-rich conditions we observed a clean surface and the growth rate increased linearly with increasing Ga flux. Under strongly Ga-rich growth conditions we observed Ga droplets on the surface and a growth rate independent of the Ga flux, so in this regime the growth is limited by the amount active nitrogen. The graph in Fig. 2 is in excellent agreement with the classical papers on the kinetics of PA-MBE of GaN [9]. The highest growth rate achieved under these growth conditions was 3 μm/h, which is in agreement with the earlier Riber results for that type of the source on thin GaN layers [8].

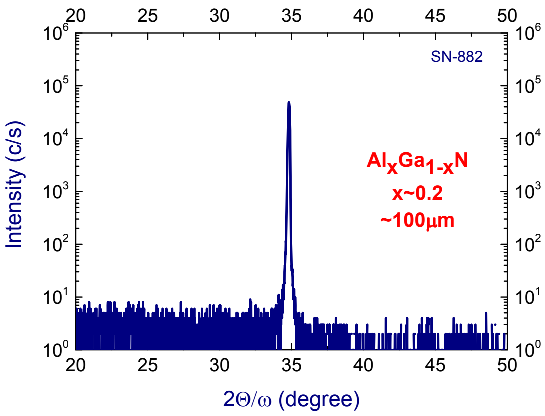

Figure 3 2θ-ω XRD scan of the 0002 peak for a wurtzite $Al_xGa_{1-x}N$ layer (x~0.2; thickness ~100 μm).

After establishing of the position of transition from N-rich to Ga-rich growth we have grown a set of wurtzite $Al_xGa_{1-x}N$ layer under slightly group III-rich conditions with the different thickness and different Al content. We used 2-inch (0001) sapphire and (111)B GaAs substrates. Figure 3 shows a 2θ-ω XRD plot for a ~100 μm thick wurtzite $Al_xGa_{1-x}N$ with x~0.2. In XRD studies we have observed a single 0002 peak at ~35 degrees, which is in the correct position for a wurtzite $Al_xGa_{1-x}N$ layer. Using Vegard's law, we can estimate the composition of the $Al_xGa_{1-x}N$ layer shown in Fig. 3 to be x~0.2. The value of AlN fraction in this $Al_xGa_{1-x}N$ layer was also confirmed by SIMS and EDX measurements. The full-width-at-half - maximum (FWHM) of the 0002 peak at ~35° from XRD ω-plot for $Al_xGa_{1-x}N$ layer shown in Fig. 3 is about 0.3°. From high resolution XRD scans we can estimate the zinc-blende fraction, which in this case was below our detection limit (<0.1%). This data confirms that we are able to sustain the same good structural quality of wurtzite $Al_xGa_{1-x}N$ layers, whilst increasing the thickness from the very thin layers up to ~100 μm. This is a very significant result, because it shows that MBE can be a viable method for the growth of bulk free-standing wurtzite $Al_xGa_{1-x}N$ crystals.

We have investigated reciprocal space maps and rocking curves for this series of samples and observed a gradual increase in FWHM ω and a decrease in XRD peak intensity with increasing AlN fraction in $Al_xGa_{1-x}N$ layers from 0 to x~0.5. The intensity of the XRD peak remains strong and the FWHM ω is relatively narrow for all $Al_xGa_{1-x}N$ layers.

The depth uniformity of Al incorporation in the $Al_xGa_{1-x}N$ layers was studied using SIMS. Figure 4 shows SIMS profiles for Al, Ga, and N at the centre of the 2-inch $Al_xGa_{1-x}N$ layer. The thickness of the layer is >8 μm and Al content is x~0.2. We observed a uniform distribution of

Al, Ga and N within the bulk of $Al_xGa_{1-x}N$ layers. In Fig. 4 we show data for a relatively thin $Al_xGa_{1-x}N$ layer in order to decrease the SIMS sputtering time, but the general trends will remain valid for the thicker layers. There is no significant As incorporation into the bulk of $Al_xGa_{1-x}N$ layer, which was confirmed by the fact that the As signal is at the background level of the SIMS system.

We have grown $Al_xGa_{1-x}N$ layers on GaAs substrates and subsequently removed the GaAs using a chemical etch in order to achieve free-standing $Al_xGa_{1-x}N$ wafers. At a thickness of ~30 µm, free-standing GaN wafers can easily be handled without cracking. Therefore, bulk $Al_xGa_{1-x}N$ wafers with thicknesses in the 30-100 µm range may be used as substrates for further growth of $Al_xGa_{1-x}N$ -based structures and devices. Our novel high efficiency RF plasma source allowed us to achieve such $Al_xGa_{1-x}N$ thicknesses on 2-inch wafers in a single day's growth, which makes our bulk growth technique commercially viable.

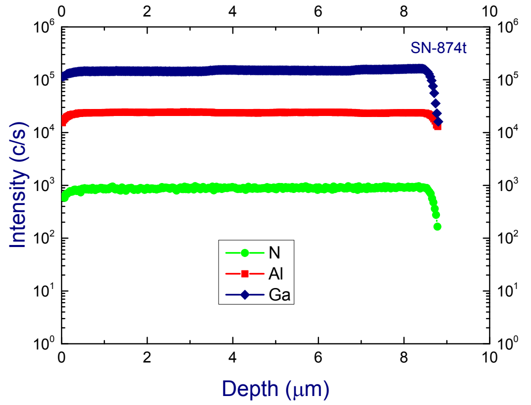

Figure 4 SIMS profiles for Al, Ga and N for a w-$Al_xGa_{1-x}N$ layer (x~0.2).

4 Summary

We have studied the growth of free-standing wurtzite $Al_xGa_{1-x}N$ bulk crystals by PA-MBE. With the novel Riber source with the 5880 holes aperture plate, we have demonstrated growth rates of $Al_xGa_{1-x}N$ up to 3 µm/h. Wurtzite (hexagonal) $Al_xGa_{1-x}N$ films with an Al content up to x~0.5 and thicknesses up to 100 µm were grown by PA-MBE on 2-inch sapphire and GaAs (111)B substrates. Bulk $Al_xGa_{1-x}N$ wafers with thicknesses in the 30–100 µm range may be used as substrates for further growth of $Al_xGa_{1-x}N$ -based structures and devices. Our novel high efficiency RF plasma source allowed us to achieve such $Al_xGa_{1-x}N$ thicknesses in a single day's growth, which makes our $Al_xGa_{1-x}N$ bulk MBE growth technique commercially viable.

Acknowledgements This work was undertaken with support from the EPSRC (EP/K008323/1). We want to acknowledge Loughborough Surface Analysis Ltd for SIMS measurements and discussions of results.

References

[1] J. H. Edgar, S. Strite, I. Akasaki, H. Amano, and C. Wetzel, Eds., Gallium Nitride and Related Semiconductors (INSPEC, Stevenage, 1999), ISBN 0 85296 953 8.
[2] A.Belousov, S. Katrych, J. Jun, J. Zhang, D. Gunther, R. Sobolewski, J. Karpinski, and B. Batlogg, J. Cryst. Growth **311,** 3971 (2009).
[3] Y.V. Melnik, V.A. Soukhoveev, K.V. Tsvetkov, and V.A. Dmitriev, MRS Symp. Proc. **764,** 363 (2003).
[4] S. V. Novikov, N. M. Stanton, R. P. Campion, R. D. Morris, H. L. Geen, C. T. Foxon, and A. J. Kent, Semicond. Sci. Technol. **23,** 015018 (2008).
[5] S. V. Novikov, C. R. Staddon, R. E. L. Powell, A. V. Akimov, F. Luckert, P. R. Edwards, R. W. Martin, A. J. Kent, and C. T. Foxon, J. Cryst. Growth **322.** 23 (2011).
[6] B. M. McSkimming, F. Wua, T. Huault, C. Chaix, and J. S. Speck, J. Cryst. Growth **386.** 168 (2014).
[7] S. V. Novikov, C. R. Staddon, R. W. Martin, A. J. Kent, and C. T. Foxon, J. Cryst. Growth **425.** 125 (2015).
[8] B. M. McSkimming, C. Chaix, and J. S. Speck, J. Vac. Sci. Technol. A **33**, 05E128 (2015).
[9] B. Heying, R. Averbeck, L.F. Chen, E. Haus, H. Riechert, and J.S. Speck, J. Appl. Phys. **88,** 1855 (2000).